FINE STRUCTURES IN SUNSPOTS

M. SOBOTKA
Astronomical Institute of the Academy of Sciences
CZ-25165 Ondřejov, Czech Republic

Abstract. A review of the present knowledge on fine-scale features in sunspots at the photospheric level is given. The principal aim is to summarize and discuss the results of observations with high spatial resolution but also several important theoretical models are briefly described.

1. What is a Sunspot?

1.1. HISTORICAL OBSERVATIONS

Many centuries ago people noticed that our life-giving star, the Sun, sometimes showed dark spots on its radiating surface. Records on occasional naked-eye observations, covering an interval of about 18 centuries, can be found in Chinese chronicles. In Europe, large sunspots were sometimes misinterpreted as transits of Mercury or Venus across the Sun. The situation changed after the introduction of the telescope in astronomy around 1609. The first telescopic observations of sunspots were probably made by T. Harriot in 1610. However, the first person who published this discovery was J. Fabricius. His small book *Maculae in Sole observatis* appeared in 1611. In the same year, C. Scheiner and J.B. Cysat saw sunspots through the smoke rising from the burning university's tower. They observed many sunspots later, but they still were not sure if the spots were really connected to the solar surface. This question was answered by Galileo, who observed sunspots for the first time in 1611, too, and measured the positions and motions of sunspots over the solar disk which he explained by a rotation of the sun.

An important discovery was announced by A. Wilson in 1769. He noticed that the penumbra of a circular sunspot near the solar limb was narrower on the center side than that on the limb side. He inferred correctly that the umbra was located deeper than the solar photosphere. The difference in heights is nowadays called *Wilson depression*. Statistical rules of sunspots' occurence and the solar cycle were discovered in following decades, particularly in 19^{th} century. This way, sunspots became the first observed phenomena of the whole complex of solar activity.

1.2. MAGNETIC FIELD IN SUNSPOTS

The modern age in the studies of sunspots began shortly after 1900 with the application of spectroscopy. First, G. E. Hale derived from intensities of spectral lines that the temperature in sunspots is lower than in the photosphere. Two years later, by measuring Zeeman splitting of magnetically sensitive absorption lines, he found that strong magnetic fields are present in sunspots (Hale, 1908). According to contemporary measurements (see, e.g., Martínez-Pillet, 1997), the magnetic field of a large spot has a maximum value approaching 3000 G at the center of the umbra. The field strength decreases monotonically outwards. Its inclination to the normal increases from zero at the center to about 40° at the umbra/penumbra boundary and about 70° at the outer edge of the penumbra.

Why are the sunspots cooler than their surroundings? According to Cowling (1934), sunspots are formed by tubes of magnetic flux breaking through the solar photosphere. On the basis of this assumption Biermann (1941) suggested that the coolness of sunspots could be explained in terms of restriction of convection by the magnetic field. Hoyle (1949) indicated that convective motions are suppressed across but not along the magnetic field lines. Thus, since the field lines fan out with height near the solar surface, the heat flux is spread over a greater area and therefore the photosphere of the spot will appear cooler. All these concepts constitute the basic assumptions for almost all sunspot models constructed until now.

1.3. MAGNETOHYDROSTATIC EQUILIBRIUM

The problem of an equilibrium of vertical magnetic field embedded in a stratified atmosphere (Priest, 1982), is a simple but very instructive quantitative example. It helps to understand the basic properties of sunspots as well as complex theoretical models.

Let the magnetic field $B(R)$ be constant with height z, having the maximum value B_i on the vertical axis $R = 0$, and $B \to 0$ for large R (R is the horizontal distance from the axis). The corresponding pressure stratifications on the axis and far from it are $p_i(z)$ and $p_e(z)$, respectively. Then, the conditions of horizontal and vertical pressure balances are

$$p(R, z) + B^2(R)/2\mu = p_e(z) \tag{1}$$

and

$$\frac{\partial p}{\partial z} = -\rho(z)g, \tag{2}$$

where μ, ρ, and g are magnetical permeability, gas density, and gravitational acceleration, respectively. Particularly, far from the axis we have

$$\frac{\mathrm{d}p_e}{\mathrm{d}z} = -\rho_e(z)g \tag{3}$$

and on the axis

$$p_i(z) + B_i^2/2\mu = p_e(z) \tag{4}$$

and

$$\frac{\mathrm{d}p_i}{\mathrm{d}z} = -\rho_i(z)g. \tag{5}$$

Differentiating (4) we see that the pressure gradients $\mathrm{d}p_e/\mathrm{d}z$ and $\mathrm{d}p_i/\mathrm{d}z$ are equal, and from (3) and (5) it follows that

$$\rho_i(z) = \rho_e(z). \tag{6}$$

Moreover, from (4) we see that p_i (inside a sunspot) is smaller than p_e (outside) and, introducing the ideal gas equation of state, we can calculate the ratio of internal and external temperatures:

$$\frac{T_i(z)}{T_e(z)} = 1 - \frac{B_i^2}{2\mu p_e(z)}. \tag{7}$$

Thus, the vertical magnetic field does not influence the density but creates deficits of pressure and temperature inside the magnetized region. These deficits are necessary for the horizontal mechanical equilibrium.

According to (4), magnetic pressure $B_i^2/2\mu$ inside a vertical magnetic field tube should be smaller than the external gas pressure $p_e(z)$. This might be true for deep subphotospheric regions but at the level of the photosphere the magnetic pressure is usually larger than $p_e(z)$. The horizontal equilibrium is perturbed and the tube diverges, increasing its radius with height. As a consequence, the magnetic field strength B_i decreases with z and, according to (4), the pressure gradient inside the tube is higher than the gradient outside. This results – see (3) and (5) – in smaller density inside the tube ($\rho_i(z) < \rho_e(z)$). This density deficit in sunspots is partially responsible for the Wilson depression.

1.4. PHYSICAL MODELS OF SUNSPOTS

The ideal sunspot model should be a dynamic one. It should describe time-dependent processes like the formation and decay of a spot, as well as temporal and spatial fluctuations of brightness and velocity in the umbra and penumbra. Unfortunately, such a model cannot be constructed at present. The main difficulties are related to the time dependence and non-local effects. The most usual approach at this moment is the magnetostatic approximation, which, within some limitations, can give a plausible figure of the global sunspot structure. Let us make a brief overview of existing magnetostatic models, based on the review by Jahn (1997).

Similarity models. The main assumption of this type of models is that the distribution of the magnetic flux (or the function $B(R)$) is similar at each height. Once the functional form of the distribution is chosen in a convenient form, the description of the magnetic field configuration can be obtained analytically (e.g. Schlüter and Temesváry, 1958).

Chanelling models. They are based on Hoyle's idea that the heat transport occurs mainly along the magnetic field lines, in channels, which diverge with height. Both the channeling of the heat flux and suppression of convective energy transport are taken into account in such models (Chitre and Shaviv, 1967).

2-D magnetostatic equilibria. If the gas pressure distribution with height is known from a model atmosphere, the magnetic field configuration can be computed solving directly the equations of magnetostatic equilibrium in two dimensions (R, z). In this way, Pizzo (1986) constructed models of sunspots of different sizes, partially based on data provided by semiempirical models.

Cluster model. As proposed by Obridko (1975) and Parker (1979a,b), subphotospheric layers of sunspots can be formed by a dynamic clustering of small magnetic tubes among which some convection may operate in a field-free plasma. Then, the observed heat flux could be transported to the surface by small field-free hot columns. This model offers a direct interpretation of umbral fine structures, particularly of umbral dots (Choudhuri, 1992).

Current sheet models. The most advanced representative of this class is the tripartite model (Jahn and Schmidt, 1994). In this model, all magnetic forces are confined to two concentric current sheets (regions permeated by electric currents that substantially contribute to the lateral balances of forces), which divide the space into three regions: the umbra, the penumbra, and the solar convective zone. The umbra is thermally isolated from the surrounding penumbra by the inner current sheet. Inside the cool umbra, the heat is transported to the photospheric level by oscillatory and overturning convection. The outer current sheet between the penumbra and the convective zone permits a lateral heat exchange via a hypothetical convection by interchanging magnetic flux elements, so that the penumbra receives 60–70% of its thermal energy from the adjacent convective zone.

1.5. THERMAL STRUCTURE AND SEMIEMPIRICAL MODELS OF SUNSPOTS

The physical state of the sunspot atmosphere (i.e. the temperature, pressure, density, magnetic and velocity fields) is usually determined by semiempirical modelling. The word "semiempirical" means that in addition to empirical observations (intensities in spectral lines and continuum), some theoretical assumptions (hydrostatic equilibrium, magnetic geometry, atomic physics, number of atmospheric components etc.) have to be taken into account. Semiempirical modelling generally involves radiative transfer calculations and model atmosphere construction, coupled in a "manual" or automated trial-and-error loop: Computed line profiles and continuum intensities are compared to the observed ones and the model atmosphere is changed until a satisfactory fit is achieved.

Since sunspots are dark, their radiation, after passing through the Earth's atmosphere, is always contaminated by *stray light* originating in the much brighter surroundings. Generally,

$$I_{obs} = I + \alpha I_s, \tag{8}$$

where I_{obs} and I are observed and "true" intensities in the sunspot, I_s stands for an intensity in the surroundings of the spot, and α is a fraction of stray light. The value of α is dependent on meteorological conditions, position of the spot on the solar disk, local distribution of brightness around the observed region, and, last but not least, on the instrument. It is very difficult to determine it with sufficient accuracy. To get acquainted with this problem we refer the reader to the papers by Zwaan (1965), Martínez-Pillet (1992), and Bonet (this book).

Many semiempirical models of sunspots have been constructed until now (see reviews by Maltby, 1992 and Solanki, 1997). Here we would like to mention the set of 3 models published by Maltby et al. (1986), which has become a standard in the last decade. The models are constructed for the darkest parts of umbrae and correspond to the early, middle, and late phases of the solar cycle. They cover the range of heights between -120 and 2100 km (0 km is defined at $\tau_{5000} = 1$), which includes the photosphere and the chromosphere above the umbra. The temperature distributions with height are shown in Figure 1. It can be seen that the photospheres of large umbrae get warmer during the solar cycle.

Two model atmospheres, corresponding to hot (small) and cool (large) umbrae, were computed recently by Collados et al. (1994). These are the first models for which a simultaneous determination of the magnetic field and thermal stratification is presented.

The temperature (or the brightness) is a function of position within the umbra and the penumbra. This follows directly from high-resolution

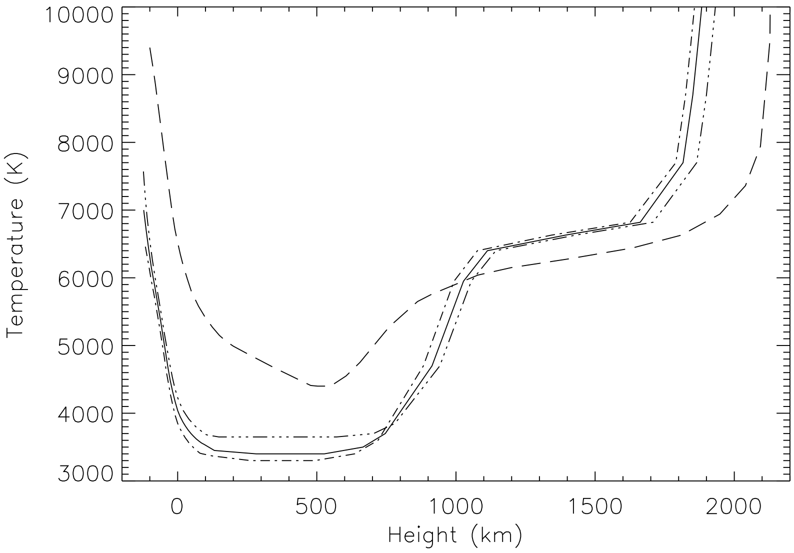

Figure 1. Temperature vs. height in umbral models by Maltby et al. (1986) for the early (dash-dot), middle (solid), and late (dash-3dots) phases of the solar cycle, and in the quite sun (long dash). Zero heights correspond to the levels $\tau = 1$ in each model separately.

imaging of sunspots, but also from low-resolution spectroscopic observations, where some lines of ionized metals cannot be explained in terms of a homogeneous model (Mallia and Petford, 1972). To involve, at least roughly, the spatial variations of temperature in the model atmosphere, two-component models have been constructed. The models of the bright and dark components (e.g. umbral dots and dark background in the umbra; bright and dark filaments in the penumbra) are computed separately. Then, the outgoing intensity is calculated as a mixture of radiations from both models:

$$I_{obs} = (1 - \beta)I_d + \beta I_b + \alpha I_s, \tag{9}$$

where the subscripts d and b denote the dark and bright components, respectively, and β is the *filling factor*, defined as the ratio of the total area of the bright component to the total area under investigation (e.g. the umbral area). The term αI_s corresponds to stray light.

For more details we refer again the reader to the reviews by Maltby (1992) and Solanki (1997). The most comprehensive umbral two-component model is that by Obridko and Staude (1988). It ranges from the photosphere to the transition region. The filling factor β is 5–10%, which is typical for many umbrae. In the last years, with the development of high-resolution observing techniques and 2-D spectroscopy, the classical two-component modelling is loosing its rôle in the studies of sunspot fine structures, but it should be considered as an important tool for the interpretation of polarimetric measurements and the investigation of small, partially unresolved features.

2. Morphology and Global Parameters of Sunspots

2.1. FIRST HIGH-RESOLUTION OBSERVATIONS

Observations of sunspots with high spatial resolution have a long history. In 1870 appeared the first edition of a fundamental work in solar astronomy by P. A. Secchi: *Le Soleil.* Most of the basic concepts of the sunspots' morphology can be found there. Secchi made his visual observations from 1865 to 1870 with a resolution approaching to 0".3 in some cases. In his wonderful drawings he presented not only the basic morphological features like multiple umbrae, light bridges, and penumbral filamentary structure, but also "knots" in bright penumbral filaments (penumbral grains) and internal structure of light bridges. He also noticed spatial variations in umbral brightness and the darkest regions –"holes"– in the umbra (dark nuclei). In three of his drawings even some umbral dots can be seen, although he did not describe them.

A large collection of sunspot photographs with spatial resolution of 0".7–1" was published by Chevalier (1916). The presence of many visually observed structures was confirmed there and, moreover, a small-scale granular-like pattern in the umbra was observed. The existence of "umbral granulation" was confirmed later by several observers (Thiessen, 1950; Rösch, 1957; Bray and Loughhead, 1964; Bumba et al., 1975). Bumba and Suda (1980) claimed that the spatial distribution of "granules" inside the umbra is identical with that in the photosphere.

A new concept was introduced by Danielson (1964). In the set of photographs from the balloon-borne experiment Stratoscope he detected very small, bright point-like features that he called "umbral dots". The spatial distribution of umbral dots was quite different from the photospheric granulation pattern. Since that moment, there were two parallel concepts, umbral granulation and umbral dots, concerning probably the same effect. This ambiguity was resolved during the 1980s, when new instruments and observing techniques made it possible to get systematically images with a resolution below 0".5. It seems now that umbral granules corresponded to groups and clusters of umbral dots, detected in lower-resolution observations (0.5"–1"), and that the partially resolved umbral intensity pattern resembled apparently the photospheric granulation.

2.2. AN OVERVIEW OF SUNSPOT FINE STRUCTURES

Let us summarize the nomenclature of the basic fine structure elements according to contemporary observations. See also the illustration in Figure 2.

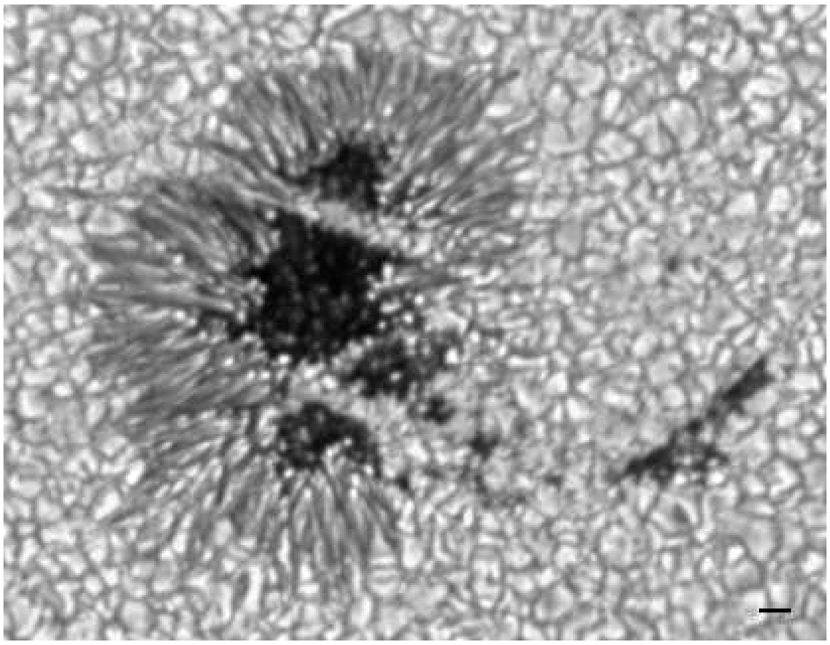

Figure 2. White-light image of the sunspot NOAA 7519 showing umbral cores, dark nuclei, umbral dots (UDs), light bridges (LBs), penumbral grains (PGs), and dark fibrils. The bar in the lower right corner is 2" long. (Courtesy P.N. Brandt., G.B. Scharmer, and G.W. Simon, Swedish Vacuum Solar Telescope, La Palma.)

In many sunspots, instead of a single umbra, we observe multiple umbrae, which seem to behave like independent units. These are termed *umbral cores*, reserving the more general term umbra for the entirety of dark areas in the spot. Umbral cores are basic umbral structures which survive the whole lifetime of the spot. From the phenomenological point of view, umbral cores consist of two components. The dark one looks like a coherent background with smoothly varying intensity forming brighter and darker regions with diffuse transitions. For this reason we call it *diffuse background*. The well-distinguished darkest regions (local intensity minima) are called *dark nuclei*. The bright component, embedded in the diffuse background, is formed by *umbral dots* (UDs) or clusters of them and by faint light bridges.

Light bridges (LBs) show a large variety of sizes, brightnesses, and shapes. Some of them separate umbral cores, being a substantial part of the sunpots' configuration, others are located inside umbral cores, forming, together with UDs, the umbral bright component. Several attempts were made to establish a morphological classification of LBs (for example Bray and Loughhead, 1964; Muller, 1979; Bumba and Suda, 1983). Here we present a simple two-dimensional classification based on two parameters: (i) The general morphology related to the sunspot configuration, namely, if the LB separates umbral cores (strong LB) or not (faint LB). (ii) The internal structure (granular or filamentary). Thus, four basic types of LBs are distinguished: faint-granular (FG), faint-filamentary (FF), strong-granular (SG), and strong-filamentary (SF).

The penumbra of sunspots is formed by *bright filaments* separated by narrow *dark fibrils*. In a regular spot the filaments cross the penumbra in almost radial direction. Young and irregular spots often develop only parts of the penumbra. Sunspots without the penumbra are usually called *pores*. Bright filaments are, in fact, chains of aligned *penumbral grains* (PGs). On the inner penumbral boundary, some PGs penetrate into the umbra as *penumbral extensions*.

2.3. GLOBAL PARAMETERS

Global parameters of sunspots, like the size, minimum intensity, and magnetic field, are mostly related to umbral cores. As we already mentioned, each umbral core behaves as an independent unit of the umbra, so that the parameters may differ strongly from one umbral core to another even in one sunspot. In this case, the largest (and usually also the darkest) one is taken as a representative of the whole spot.

An important photometric parameter of umbral cores is the minimum intensity (or the intensity of the darkest point) I_{min}, which is usually in the range 0.05–0.3 of the mean photospheric intensity at $\lambda \simeq 5400$Å. It is well correlated with the average intensity of the diffuse background (Sobotka et al., 1993). This correlation, which is not obvious due to a significant inhomogeneity of the background intensity, allows to characterize the entire brightness of the diffuse background by a single, easily measurable value.

Let us now consider the relations between the umbral brightness, size, and magnetic field strength. Early observations suggested that large sunspots are darker than small ones. Such observations were often insufficiently corrected for stray light, as pointed out by Zwaan (1965). Observations made since then have usually been carefully corrected for stray light and, in fact, for sunspots with umbral diameters larger than 8"–10" no significant dependence of brightness on umbral size were found (e.g. Albregtsen and Maltby, 1981). However, Sobotka (1985), using profiles of spectral lines corrected for stray light, showed that small umbrae with diameters

$D_u < 7"–8"$ have temperatures systematically higher than the large ones. More recently, Kopp and Rabin (1992) found a clear relationship between the umbral brightness at $\lambda = 1.56\,\mu$m and sunspot size. These results were confirmed independently by Martínez-Pillet and Vázquez (1993). These authors circumvent much of the stray light problem by using the Stokes V profiles of lines with different temperature sensitivities. Similar results were obtained by Sobotka et al. (1993) from high-resolution white-light images of 14 umbral cores around $\lambda = 5425$Å. The values of I_{min} increased from 0.05–0.06 ($D_u > 12"$) to 0.25–0.30 ($D_u < 8"$). Their scattering, however, did not allow to establish a clear rule for this relationship.

The relation between the magnetic field and brightness (or temperature) of umbral cores was first predicted by the theory: Regions with higher magnetic field strength B should be darker and cooler than those with lower B. This problem was extensively investigated, both theoretically and observationally, during the past four decades. The most careful and thorough studies have been made by Kopp and Rabin (1992) and Martínez-Pillet and Vázquez (1993). The latter authors, analyzing profiles of FeI and TiI lines observed in 8 sunspots, have found that the temperature decreases linearly with increasing B^2. This is valid in a general sense, i.e. when comparing different umbral cores, as well as in a local sense, i.e. at different positions inside one umbral core. For more details on this topic we refer the reader to the review by Solanki (1997).

2.4. DARK NUCLEI

The darkest regions in umbral cores are dark nuclei. According to the previous paragraph, they are the areas with the strongest magnetic field, which is nearly perpendicular to the solar surface. They are not necessarily located at the center of umbral cores – in many cases they were observed quite close to the edge of the penumbra. Few UDs are seen inside them and some dark nuclei appear void even in the best-quality frames.

Dark nuclei cover 10–20% of the total umbral core area, but in strongly fragmented umbrae during decay, as well as in small pores, they seem to be identical to umbral cores. The average size of dark nuclei is about 1".5, similar to the mean size of photospheric granules. The intensities are spread in a wide range, depending on the individual characteristics of umbral cores. Studying the relation between minimum intensities and sizes of dark nuclei we see, separately for each sunspot, a slight trend of decreasing brightness with increasing size (Sobotka et al., 1993).

3. The Penumbra

3.1. PENUMBRAL FINE STRUCTURES

The most typical feature of penumbral fine structures is the elongated shape, a consequence of the strongly inclined magnetic field. As we already mentioned, bright penumbral filaments consist of PGs (penumbral grains). Analyzing a series of high-resolution photographs taken at Pic du Midi, Muller (1973a,b) thoroughly described their characteristics: PGs have cometary-like shapes with "heads" pointing towards the umbra (see Figure 2). They appear all over the penumbra and are aligned in the form of bright filaments. The mean width of PGs is of about 0".36 (260 km) and the length is in the range 0".5–2". The observed brightness approaches the photospheric one (0.95–1, λ = 5500Å) and the lifetimes are between 40 minutes and 4 hours.

PGs are separated by narrow dark fibrils which, unlike the well-distinguishable PGs, look rather like a coherent background surrounding the bright features. The average intensity of dark fibrils is 0.6 and decreases towards the umbra (Muller, 1973b). In spite of a clear two-component structure of the penumbra, the histogram of brightnesses has a single peak and does not show any photometric evidence of two components. This can be explained by the fact that the intensities vary substantially on large scales through the penumbra. Thus, the concepts of "bright" and "dark" have only a local meaning, in the sense that a local maximum of brightness can be less bright than a minimum elsewhere (Wiehr et al., 1984; Muller, 1992). We shall see later that a similar situation occurs also in the umbra.

3.2. MAGNETIC FIELD IN PENUMBRAL FILAMENTS

Let us now turn our attention to the differences in magnetic field strength and inclination between the bright filaments and dark fibrils. This problem, which requires observations with spatial resolution better than 0".5, is very important for understanding the physical conditions in the penumbra and the Evershed effect.

The first indication was set by Beckers and Schröter (1969), who inferred from moderate-resolution observations (about 1") that the magnetic field should be more inclined, with respect to the normal, in dark fibrils than in bright filaments. High-resolution (0".32–0".5) measurements based on Zeeman splitting of spectral lines (Wiehr and Stellmacher, 1989; Lites et al., 1990) revealed some fluctuations of the magnetic field strength which, however, were uncorrelated with the changes of the continuum brightness. The lack of correlation was probably due to the difference of heights where the magnetic sensitive spectral lines and continuum were formed. Degenhardt and Wiehr (1991) circumvented this problem, using the deep-formed photospheric line Fe I 6842.7 Å. They found the magnetic field stronger by 10% and more inclined at the locations of dark fibrils, but only in a part of the penumbra.

Similar results were obtained independently from polarimetric measurements: Schmidt et al. (1992) found that the field inclination in dark fibrils was by 10^o larger than in bright filaments, but they did not find any variations in the field strength. Title et al. (1993) observed in their high-resolution magnetograms that on the average the inclination fluctuated $\pm 18^o$; the spatial scale of these fluctuations was comparable to the width of penumbral filaments. Hofmann et al. (1994) concluded from Stokes V profiles of 4 spectral lines that the magnetic field was clearly more inclined in dark fibrils. They also found an anticorrelation between the field strength and continuum brightness, i.e., stronger field in darker regions – nevertheless, the anticorrelation was non-uniform across the penumbra.

We can summarize that, according to recent observations, the magnetic field is very probably stronger and more horizontal in dark fibrils and weaker and more vertical in PGs. This statement, however, has still to be confirmed by more observations which should be made at different locations in the penumbra.

3.3. PROPER MOTIONS AND VERTICAL VELOCITIES

In movies composed of white-light images we can see that nearly all penumbral fine structures are in motion. PGs move towards the umbra with an average speed of 0.3–0.5 km/s (Muller, 1973a, 1976; Tönjes and Wöhl, 1982). Muller claimed that the speed increases with decreasing distance to the inner penumbral boundary, where it reaches its maximum. Tönjes and Wöhl, however, observed the maximum speed in the middle part of the penumbra. Some PGs cross the umbral border, decrease their velocity, and continue to move as UDs (Sobotka et al., 1995).

On the other hand, dark cloud-like features, which arise from the dark fibrils, move rapidly (up to 3.5 km/s) towards the outer penumbral border (Zirin and Wang, 1989; Shine et al., 1994). They are best observable in the middle and outer parts of penumbrae, where their size increases. The motions of dark features in the outer penumbra predominate to such a degree that the flow maps obtained as a result of the local correlation tracking show the outward motions only (Molowny-Horas, 1994). This flow pattern continues outside the penumbra, where photospheric granules located close to the outer penumbral border move away from the sunspot with velocities of about 1 km/s (Muller and Mena, 1987; Shine et al., 1987; Wang and Zirin, 1992). Most of PGs in the outer penumbra still move inwards, but some of them seem to be swept out by outward flows. One can have the impression that PGs resemble a shoal of fish swimming against a strong stream.

Vertical velocities in penumbral fine structures can be measured from Doppler shifts in high spatial resolution spectra of sunspots near the center of solar disk. Beckers and Schröter (1969) were the first who reported possible upward motions in bright filaments. Lites et al. (1990) did not find any correlation between the vertical velocities and the continuum brightness, but recently, Johannesson (1993) and Rimmele (1995a) observed upflows of 0.1–0.2 km/s in isolated PGs.

3.4. EVERSHED EFFECT

The Evershed effect is the well-known shift of spectral line cores combined with line asymmetries. It is best observable in penumbrae of spots at heliocentric angles larger than 30°. At the photospheric level, it is commonly interpreted as an almost horizontal outflow of 3–4 km/s. The Evershed effect has recently been discussed in reviews by Thomas and Weiss (1992) and Maltby (1997). Here we shall concentrate on one important question, related directly to penumbral fine structures and first posed by Beckers and Schröter (1969): Is the Evershed flow confined to dark fibrils?

The first studies (Wiehr and Stellmacher, 1989; Lites et al., 1990; Johannesson, 1993), based on high-resolution spectrograms, did not reveal any correlation between Doppler shifts and continuum intensity variations. On the other hand, filtergrams obtained by Title et al. (1993) at La Palma, and re-examined later by del Toro Iniesta et al. (1994), showed a tendency of the Evershed flow to be spatially correlated with regions of more inclined magnetic field, i.e. with dark fibrils.

Degenhardt and Wiehr (1994) and Wiehr and Degenhardt (1994) explained the discrepancy between the results based on spectra and filtergrams: From shifts of 5 magnetic insensitive lines with different formation heights they concluded that the velocity fluctuations and intensity variations have different horizontal scales at different heights in the atmosphere. They obtained a good spatial correlation between dark penumbral fibrils and enhanced wing shifts of deep-formed lines. The comparison between line core shifts and continuum variations did not give any correlation, because the continuum and the cores of lines are formed at different heights and have different scales of horizontal fluctuations.

Filtergram data analyzed by Shine et al. (1994) and Rimmele (1994, 1995a,b) have shown that the Evershed flow is confined to dark fibrils, which are nearly horizontal and parallel to the strongly inclined magnetic field. It was also found that the dark cloud-like features with outward-directed proper motions are cospatial with "Evershed clouds", outward-moving regions with a size of about 1000 km, where the Doppler velocity is enhanced, and that the Evershed effect is time-dependent.

So, the contemporary observational figure of the penumbra is based on two components: In the penumbral background, dark fibrils, the magnetic field is strongly inclined and it becomes nearly horizontal in the outer penumbra. Horizontal motions away from the sunspot are observed here in the forms of Evershed effect and proper motions as well. The bright component, PGs, has a weaker and less inclined magnetic field, its contribution to the Evershed effect is small, and the proper motions are directed into the umbra. It should be underlined, however, that the proper motions are apparent and they are not related to real plasma flows.

4. Light Bridges

4.1. PHOTOMETRIC PARAMETERS AND INTERNAL STRUCTURE

LBs, bright structures crossing the umbra or deeply penetrating into it, are important elements of sunspots' structure. They live several days, although their shape may change substantially on the scale of hours. LBs are closely related to the topology of the sunspot magnetic field (Bumba and Suda, 1983) and play an important rôle in the evolution of sunspots (Vázquez, 1973). Their photometric characteristics, morphology, and internal structure can be very different. For example, the brightness can range from the intensity of faint UDs up to the photospheric one, the width varies from less than 1" to several seconds of arc, the internal structure can be granular or filamentary etc. In the following we refer to the types of LBs according to the classification presented in Section 2.2 and summarized in Table 1.

Faint LBs (types FG, FF) belong to the bright component of umbral cores. LBs of type FG are narrow (0.5–2") bright streamers embedded in the diffuse background, usually connected to the penumbra by one of their ends. They consist of small bright grains similar to UDs. The average observed brightness and size of bright grains are 0.5–0.7 and 0".47, respectively, and the mean nearest neighbour distance between the centers of the grains is 0".53. The grains cover about 50% of the total area of the LB (Sobotka et al., 1993). Type FF bridges consist of moving elongated bright grains (speed of proper motions up to 0.5 km/s, lifetime $>$ 50 minutes), which are very similar to PGs (Muller, 1979).

Strong LBs (types SG, SF) are located between two or more umbral cores. Usually, type SG separates umbral cores of equal magnetic polarities and type SF those of opposite polarities (Casanovas et al., 1974; Bumba and Suda, 1983). However, exceptions of this rule were observed, when a SF bridge was located between umbral cores of equal polarities (Bumba and

TABLE 1. Classification of light bridges

	Granular	**Filamentary**
Faint *(located inside umbral core)*	**FG** aligned bright grains	**FF** intrusions of penumbra
Strong *(separating umbral cores)*	**SG** photospheric-like granules	**SF** (distorted) parts of penumbra

Suda, 1983; Rüedi et al., 1995). Sobotka et al. (1994) analyzed 2-D power spectra of intensity fluctuations inside two LBs of type SG, together with simultaneously observed profiles of the line Fe I 5434.5 Å. They found that the typical size of LB granules was 1".2, which is smaller than in the quiet granulation (1".5). The slopes of power spectra indicated the presence of a Kolmogorov turbulent cascade, with an exception of a peak at scales of 0".5. This peak reflected the presence of small bright grains, clearly visible in the LBs, with a mean nearest neighbour distance of 0".5 (slightly less than in type FG). Two of these small bright grains, together with a dark lane between them, were resolved spectroscopically. The line shifts (upflows of 0.25 km/s in the bright grains with respect to the dark lane) and bisector shapes indicated a convective origin of these structures.

4.2. MAGNETIC FIELD IN LIGHT BRIDGES

Beckers and Schröter (1969) found that the magnetic field was by 200–300 G lower and more inclined to the horizontal than in the neighbouring umbra. Abdusamatov (1970) determined from magnetographic observations a much larger decrease of the magnetic field strength in a SG bridge. A field reduction of 800 G was found by Kneer (1973). Lites et al. (1991) determined an upper limit to the magnetic field strength of approximately 1000 G in a SG bridge, while the maximum field strength in a nearby umbral core was 2300 G. Wiehr and Degenhardt (1993) reported reduced and more inclined magnetic field in a strong LB.

Rüedi et al. (1995) investigated a SF bridge between two umbral cores of equal polarity using Fe I lines at $\lambda = 1.56\,\mu$m with moderate spatial resolution (1"–2"). From the inversion of Stokes I and V profiles they obtained magnetic field strength up to 3250 G in the umbra and 2000 G in the LB. The inclination of magnetic field in the LB was similar to that in the penumbra (70°). At some locations a downflow up to 1.5 km/s was seen in the LB relative to the umbral material. A comprehensive paper on physical conditions in LBs was recently published by Leka (1997). She obtained the magnetic field reduction 500–1200 G relative to the umbra and the field inclination larger than in the umbra but smaller than in the penumbra. The field azimuth was aligned with the axis of LBs. Both upflows and downflows of 0.4 km/s were observed.

We can say that recent observations indicate that magnetic field strength in strong LBs is substantially lower than in adjacent umbra. Similarly, some reduction of magnetic field we can expect also in faint LBs. This fact, together with our knowledge of LBs' internal structure and evolution, can be used as a proof that LBs are "deep" structures, formed due to large-scale inhomogeneities in sunspots' magnetic configuration, and not merely superficial phenomena.

4.3. EVOLUTION OF LIGHT BRIDGES

The evolution of LBs is strongly related to the development of the whole sunspot. It was observed several times (Vázquez, 1973; Adjabshirzadeh and Koutchmy, 1980; Kusoffsky and Lundstedt, 1986) that chains of long-lived UDs develop into FG bridges. Then, a faint LB can increase the width and brightness until the umbral core splits and a strong LB appears (Rüedi et al., 1995). Finally, during the sunspot's decay phase, SG bridges develop into regions of photospheric granulation which push away the umbral cores (Vázquez, 1973). In case of formation of a large spot a reverse process can take place: Strips of photospheric material compressed between approaching umbrae are squeezed into SG bridges and, similarly, some parts of penumbra are converted into SF bridges.

Since we know that the magnetic field strength in LBs is lower than in the surrounding umbra and we can expect intuitively that weaker magnetic field permits a more efficient transport of heat from below, we can imagine the following scenario: A local weakening of the magnetic field first gives rise to stable chains and clusters of UDs or to faint LBs. Once the magnetic field begins to decrease, more thermal energy is transported upwards, larger convective cells can be formed, the region brightens, and a strong LB appears. This is the first step towards the re-establishment of the photospheric conditions, which, if the magnetic field continues to weaken, leads to the decay of the sunspot and to the onset of photospheric convection, i.e. to the formation of granulation.

5. Umbral Dots

5.1. BRIGHTNESS AND SIZE

UDs are the most challenging objects of sunspot fine structure. Excellent seeing and a nearly perfect telescope of at least medium size (resolution limit $\leq$ 0".3) are necessary to observe them. Since UDs are observed near the resolution limit of contemporary telescopes, their observed brightnesses and sizes differ from the real ones.

One possibility how to estimate the "true" intensity J and diameter d from the observed quantities I and D is a simultaneous photometry in two wavelengths (e.g. blue and red). Both the observed and "true" intensities of an UD can be expressed through the diffuse background intensities (I_λ^{db}, J_λ^{db}), which are supposed to be known, and the UD's surplus intensities (ΔI_λ, ΔJ_λ):

$$I_\lambda = I_\lambda^{db} + \Delta I_\lambda, \;\; J_\lambda = J_\lambda^{db} + \Delta J_\lambda, \;\; \lambda = blue,\, red \tag{10}$$

From the flux conservation law it follows that

$$\Delta I_\lambda D_\lambda^2 = \Delta J_\lambda d_\lambda^2, \;\; d_{blue} = d_{red} \tag{11}$$

and ΔJ_{blue} can be expressed through ΔJ_{red} using the colour index c :

$$\Delta J_{blue} = c \Delta J_{red}, \;\; c = \frac{\Delta I_{blue} D_{blue}^2}{\Delta I_{red} D_{red}^2} \tag{12}$$

The colour index can be calculated from observed values. Finally, we obtain a system of two equations for the "true" intensity ΔJ_{red} and the colour temperature T:

$$J_{blue} = J_{blue}^{db} + c\Delta J_{red} = B_{blue}(T)/I_{blue}^{ph} \tag{13}$$

$$J_{red} = J_{red}^{db} + \Delta J_{red} = B_{red}(T)/I_{red}^{ph}. \tag{14}$$

The expression $B_\lambda(T)/I_\lambda^{ph}$ is the Planck function in units of the mean photospheric intensity. The "true" diameter d can be calculated from (11).

First estimates based on non-simultaneous exposures in blue and red gave $J \simeq I^{ph}$ and $d \simeq$ 0".14–0".28 (100–200 km) for bright UDs (Beckers and Schröter, 1968; Koutchmy and Adjabshirzadeh, 1981). These results were widely accepted for nearly two decades but more recent observations with strictly simultaneous exposures and more UDs in the sample revealed the "true" intensities and diameters to be in a broader range: Intensities often smaller than I^{ph} and $d \simeq$ 0".15–0".60 (Aballe Villero, 1992). Broad ranges of "true" intensities and sizes were also reported by Grossmann-Doerth et al. (1986) and Lites et al. (1991), who analyzed white-light images restored for the estimated instrumental point-spread functions.

High spatial resolution spectra made it possible to derive the real brightnesses and sizes of UDs from local two-component semiempirical models (Sobotka et al., 1992). Observed profiles of temperature-sensitive lines in several UDs were fitted by a mixture of synthetic profiles computed from two model atmospheres, corresponding to the UD and to the adjacent dark background. In this case, the filling factor was related to the "true" size of the UD and to the spatial resolution of the observation. This method was applied later to more spectra and used to calibrate a photometric sample of 1507 UDs observed in white-light images (Sobotka et al., 1993). The result was that *the real brightness of UDs is proportional to the local brightness of the surrounding diffuse background:* On average,

$$J \simeq 3 \times J^{db}. \tag{15}$$

Analogously to the situation in the penumbra, also in the umbra the concepts of "bright" and "dark" have only a local meaning – the diffuse background at the periphery of the umbra can be brighter than UDs located inside the dark regions.

Assuming that J^{db} is known (after the stray light correction), d can easily be calculated from the flux conservation law (11). This way, for the set of 1507 UDs with observed average $\overline{D} = 0''.43 \pm 0''.1$, a "true" $\overline{d} = 0''.31 \pm 0''.09$ was obtained. *The size and brightness of UDs are uncorrelated.*

New measurements of *observed* brightnesses and sizes of 662 UDs were made by Sobotka et al. (1997a,b) in a 4.5 hour time-series of white-light images obtained at the Swedish Vacuum Solar Telescope, La Palma (Simon et al., 1994). An identification and tracking algorithm was used to determine intensities, diameters, lifetimes, and positions of UDs independently from the human factor. "Light curves" of UDs displayed mostly irregular variations, but possible periods of 32, 16, 11 minutes and shorter were also detected. The statistical distribution (histogram) of D did not show any "typical" size of UDs in the range 0".28–0"9. In fact, *the number of UDs strongly increased with decreasing D* down to the resolution limit.

5.2. LIFETIME

Lifetimes can be determined from time-series of frames. This task is quite difficult because it is not easy to identify a certain UD in different frames. The first estimates led to about 25 minutes (Beckers and Schröter, 1968; Adjabshirzadeh and Koutchmy, 1980). More recent observations made by Kitai (1986) and Kusoffsky and Lundstedt (1986) indicated that the typical lifetime was longer: 40 and 60 minutes, respectively. On the other hand, Ewell (1992) reported the mean lifetime of only 15 minutes. Several UDs were observed to exist for more than 2 hours (Kusoffsky and Lundstedt, 1986; Ewell, 1992). The time resolution of all above mentioned observations was not better than 5 minutes.

Sobotka et al. (1997a) obtained lifetimes of 662 UDs from a 4.5 hour series with a time resolution of 45 seconds. They found that 66% of UDs had lifetimes shorter than 10 minutes, 27% between 10 and 40 minutes, 6% between 40 and 120 minutes and 1% of the UDs existed longer than 2 hours. They did not find any "typical" value; rather, *the shorter the lifetime of UDs, the more numerous they were.* The lifetimes were uncorrelated with the time-averaged brightnesses of UDs, but the minimum size of UDs rose with increasing lifetime.

5.3. SPATIAL DISTRIBUTION

UDs can be found everywhere in the umbra. Their distribution, however, is not uniform. They form clusters and alignments at some "preferred" locations in the umbra and they are almost missing in dark nuclei. From measurements in 18 different umbral cores it was found that the nearest neighbour distance of UDs (0".5–0".75) decreases and the number of UDs per arcsec^2 (0.45–1.3) increases with increasing brightness of the diffuse background (Sobotka et al., 1993).

We see that UDs are more numerous and have higher average intensity in bright umbral cores compared to dark ones. The "true" filling factor β, based on "true" diameters, is 3–5% in dark umbral cores and 5–10% in bright ones. Using these typical values of β and formula (15), we can calculate the contribution of UDs to the mean umbral brightness: In dark umbral cores UDs generate about 10% of the total energy flux. In bright umbral cores the contribution of UDs amounts to 20%.

Large ($d > 0".4$) and long-lived ($t > 40$ minutes) UDs tend to appear in relatively bright regions of the diffuse background (Sobotka et al., 1997a), where the magnetic field strength is locally weaker. The brightest UDs are usually located at the periphery of the umbra, where the diffuse-background intensities are high. These UDs were easy to observe in the past, while those located inside the dark central parts were hard to detect. This was probably the historical reason for the division of UDs into two classes: *peripheral* and *central* (Grossmann-Doerth et al., 1986). Some peripheral UDs originate from PGs which passed through the penumbra/umbra boundary. It is difficult to say at this stage of knowledge if the peripheral and central UDs differ physically, because their statistical properties (sizes, lifetimes, and even proper motions) seem to be very similar.

5.4. PROPER MOTION

In movies created from time-series of high-resolution images one can see that many UDs, sometimes arising from or related to PGs, move toward the umbral center with an average speed of about 400 m/s (Kitai, 1986; Ewell 1992). Molowny-Horas (1994), using a more accurate method of velocity measurement, reported that the average speed of 28 UDs was 210 ± 50 m/s. Sobotka et al. (1997b) derived average proper motion velocities from positions of 662 UDs tracked in the 4.5 hour series. They found that the number of UDs decreases with increasing speed and that the velocities are grouped at 100 and 400 m/s.

Ewell (1992) observed that most of the moving UDs were located at the periphery of the umbra and suggested to distinguish between central and peripheral UDs on the basis of their proper motions – central UDs were stationary, while peripheral UDs drifted inwards. The spatial distribution of proper motion velocities obtained by Sobotka et al. (1997b), shown in Figure 3, is in contradiction to that idea: Moving and stationary UDs were found at any location in the umbral core, although UDs with lifetimes > 10 minutes were on the average faster at the periphery than in the central region. So, the division of UDs into central and peripheral on the basis of their proper motions was not confirmed.

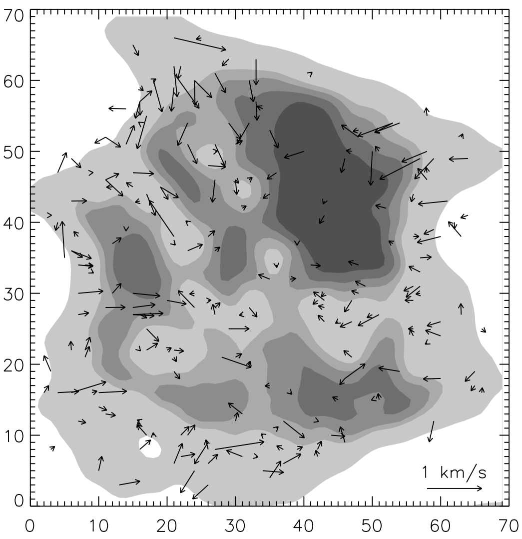

Figure 3. Vectors of proper motion velocities for 224 UDs with lifetimes longer than 10 minutes. The underlying contour image of the umbral core is an average of all frames in the time-series. Contours correspond to intensities 0.24, 0.26, 0.28, 0.30, and 0.45. One coordinate unit is 0".125 (Sobotka et al., 1997b).

Sobotka et al. (1995) observed that proper motions of UDs were influenced by the spatial distribution of dark nuclei. Most of UDs slowed down and disappeared at the borders of dark nuclei, or their trajectories were deflected. In several cases, a "collision" of moving UD or PG with a dark nucleus produced a brightening of an already existing UD on the opposite side of the dark nucleus. If the collision and subsequent brightening are physically related, e.g. by a wave propagating across the dark nucleus, the propagation speed would be about 2–7 km/s.

5.5. LINE-OF-SIGHT VELOCITY AND MAGNETIC FIELD

A significant effort was dedicated to the search of upflows or downflows in UDs. Although the spatial resolution in the spectra was better than 0".5 and velocity differences between UDs and the adjacent diffuse background were measured with an accuracy reaching 25 m/s, *no fluctuations in the line-of-sight velocities which would be spatially correlated with UDs were found* (Lites et al., 1991; Wiehr, 1994; Schmidt and Balthasar, 1994). Moreover, UDs did not display any enhancements in line asymmetries.

The magnetic field, measured with high spatial resolution from Zeeman splitting of spectral lines at locations of UDs, does not show any fine-scale fluctuations. However, *it is reduced by 1–20 % on spatial scales larger than 1"*, that is, on scales corresponding to clusters of UDs (Adjabshirzadeh and Koutchmy, 1983; Lites et al., 1991, Wiehr and Degenhardt, 1993; Schmidt and Balthasar, 1994; Tritschler and Schmidt, 1997). The vertical gradient of the magnetic field was reported to be smaller than that in the surrounding diffuse background (Wiehr and Degenhardt, 1993) or equal to that (Schmidt and Balthasar, 1994).

The absence of significant changes of line-of-sight velocities and magnetic field strength in UDs could be explained by different formation heights of spectral lines and continuum. To verify this possibility, Degenhardt and Lites (1993a,b) proposed a magnetohydrodynamical model of an "umbral flux tube", representing an UD. The shape of the umbral flux tube was similar to a bottle with a $d = 300$ km base located 200 km below the $\tau = 1$ level and a $d = 100$ km neck 300 km above $\tau = 1$. The magnetic field strength at the base was 300 G, while outside the tube, in the umbra, it was 3000 G; the temperature in the tube was 1.4 times higher than in the umbra. On the top of the model, at the neck, the magnetic field strength inside and outside the tube was equal. A stationary plasma upflow (15 m/s at the base) was present in the tube. The continuum intensity ratio J/J^{db} produced by this model was estimated to 2.5. Since spectral lines are formed at the top of the model, no magnetic field fluctuation can be detected. The diameter of the upper part of the tube is small compared to the resolution limit of contemporary telescopes, so that the observed upflow is below the error of measurement.

6. Physical Interpretation of Sunspot Fine Structures

6.1. SIMILARITIES AND RELATIONS

The observational facts presented in the previous sections give rise to many questions. For example, why are UDs, bright grains of faint LBs, and those present in strong LBs similar in observed sizes and nearest neighbour distances? Why does the nearest neighbour distance increase with decreasing brightness of umbral cores? Is there any physical relation between UDs, PGs, and bright grains in LBs? Let us summarize the similarities and relations between the fine structure elements and put them in order according to decreasing magnetic field strength in the umbra:

1. Dark nuclei are almost void of UDs. Moving UDs usually slow down and disappear at their borders.
2. The nearest neighbour distance of UDs decreases with increasing brightness of the diffuse background, that is, with decreasing magnetic field strength.
3. Large and long-lived UDs tend to appear in brighter regions of the diffuse background, where the magnetic field is weaker than in darker ones.
4. Chains of UDs can develop into granular LBs.
5. Strong granular LBs, where the magnetic field is substantially weaker than in the surrounding umbra, consist of granules smaller than but similar to photospheric ones. They also contain bright grains similar in size and nearest neighbour distance to UDs.

In regions with strongly inclined magnetic field (penumbrae and filamentary LBs) we find that:

1. Grains which form faint filamentary LBs are similar in morphology, lifetimes, and proper motions to PGs.
2. PGs which pass the penumbra/umbra boundary continue to move as UDs.

Any theory which attempts to describe the structure of sunspots and to explain the wide variety of sunspot fine structures should take into account the facts presented above. In principle, there are two basic theoretical views concerning the magnetic structure of sunspots (see e.g. the review by Thomas and Weiss, 1992): (i) A coherent but inhomogeneous flux tube, where the magnetoconvection takes place, or (ii) a tight bundle of isolated thin flux tubes, separated by field-free plasma which penetrates into layers near to the visible surface.

According to the first approach, different fine structure elements should be manifestations of different types of magnetoconvection; this will be discussed in the next subsection. In the second approach, based on the cluster model by Parker (1979a,b), UDs and, possibly, faint LBs can be explained as radiative signatures of field-free columns of hot gas intruding between the magnetic flux tubes (Choudhuri, 1986, 1992). Although these two approaches start from very different presumptions, they predict quite similar observable effects. Thus, at this moment it is practically impossible to decide from observations which model describes better the reality.

6.2. MODELS OF MAGNETOCONVECTION

Models of magnetoconvection (convection of plasma in magnetic field) are based on the solution of magnetohydrodynamical equations (see e.g. the review by Proctor, 1992). They describe the modification of plasma flows by magnetic fields and, at the same time, the changes in the magnetic field due to plasma motions. Before we present some results related directly to our topic, let us recall some specific concepts used in the theory of magnetoconvection. Many of the fundamental ideas can be comprehended within the *Boussinesq approximation* – the plasma is treated as an effectively incompressible fluid except as regards the buoyancy force.

The magnetoconvection is characterized, among others, by the *Rayleigh number* R, which is proportional to the temperature gradient ∇T, and by the *Chandrasekhar number* Q, proportional to the square of the magnetic field strength B. In the Boussinesq approximation,

$$R = \nabla T(g\alpha d^4)/(\kappa\nu), \quad Q = B^2 d^2/(4\pi\mu\rho\eta\nu), \tag{16}$$

where d is the depth of the convective cell, g the gravitational acceleration, $\alpha = T^{-1}$ is the gas expansion coefficient, ν the kinematic viscosity, and μ the magnetic permeability; η is the magnetic diffusivity, which is inversely proportional to the electric conductivity, and κ is the thermal diffusivity, inversely proportional to the density ρ (and also to the opacity).

One type of magnetoconvection is the *steady overturning convection*. It occurs when $\kappa < \eta$ and the buoyancy dominates the Lorentz force ($R \geq \pi^2 Q$). At critical $R_c = \pi^2 Q$ the convection starts as a growing instability and develops convective cells similar to those in non-magnetic regions. In the Boussinesq approximation, the temperature difference across the cell which is necessary to start the overturning convection in the subphotospheric layers of the umbra is too high (about 10^4 K/Mm for $B = 3000$ G) when compared to the thermal structure of umbrae.

Thus, another type of magnetoconvection, the *oscillatory convection*, is more probable below $\tau = 1$ in the umbra. It appears when $\kappa > \eta$. The temperature difference across the cell to start the oscillatory convection in the umbra is smaller by order than that for the overturning one. This is sufficient for the onset of the oscillatory convection in the form of surges up and down along the field lines. The efficiency of heat transport is, however, much lower than in the case of overturning convection. Under certain conditions, both types of magnetoconvection can coexist simultaneously.

6.2.1. *3-D Patterns of Magnetoconvection*

Recently, Weiss et al. (1996) and Weiss (1997) published results of a sequence of numerical experiments on an idealized model of three-dimensional nonlinear magnetoconvection. They modelled the situation in a deep stratified layer of compressible gas in an externally imposed vertical magnetic field, as in the umbra of a sunspot. The diffusivity ratio η/κ (inversely proportional to the gas density ρ) was in the range 0.2–2.2, so that oscillations were favoured at the top of the layer while overturning was favoured at its base. The simulations were computed for decreasing magnetic field strength B (decreasing Q).

When B was sufficiently large ($Q = 2000$) a *steady convection* appeared. It was characterized by a stable cellular pattern, where the isolated rising plumes were surrounded by a continuous network of sinking gas. This situation may correspond to dark nuclei without UDs, because the hot plumes are located too low to be visible.

As B decreased ($Q = 1400$) *spatially modulated oscillations* were obtained. Adjacent plumes waxed and waned alternately. The hot plumes could be observed as UDs.

For weaker fields ($Q = 1000$) an *aperiodic convection* was set on. The plumes expanded in size and the motion became more vigorous and chaotic. Magnetic structures changed as the convective pattern altered (like some "magnetic fluid"). Maybe, this situation could correspond to faint LBs.

A further reduction in B ($Q = 500$) led to a *turbulent convection* with yet larger rising hot plumes. Narrow sinking plumes with concentrated magnetic field were located at nodes in the network. This pattern may correspond to strong LBs and plages.

6.2.2. *Magnetic Flux Tube in the Penumbra*

A theoretical explanation for PGs and, possibly, for the Evershed effect was suggested by Schlichenmaier et al. (1997). They considered a 1-D thin flux tube evolving in a 2-D background – the penumbra in the tripartite sunspot model by Jahn and Schmidt (1994). The evolution was governed by the equilibrium of internal and external total (gas + magnetic) pressures, forces of gravity, buoyancy, and radiative heat exchange. The tube was formed due to interchange instability in the outer current sheet between the penumbra and the field-free quiet sun.

The scenario of the evolution is the following: Initially, the tube is in magnetohydrostatic equilibrium and lies along the inner side of the current sheet. The onset of the interchange instability is caused by radiative heating from the quiet photosphere. The heated part of the tube expands, becomes less dense, and rises upwards and inwards. The rise occurs only below the level of the photosphere where the background stratification is convectively unstable. Above the photosphere, the tube lies horizontally without motion. The footpoint, i.e. the intersection of the rising tube with $\tau = 1$, moves towards the umbra. The expansion of the tube produces a decrease of the internal magnetic pressure and, consequently, an upflow to conserve the equilibrium of total internal and external pressures. The upflow is converted into an outflow in the horizontal part of the tube.

The footpoint and the adjacent part of the tube are heated by the upflowing hot gas and they are optically thick and brighter than the background. We observe them as an inward-moving PG. Further out in the tube the outflowing gas cools down and becomes optically thin. The underlying dark background is seen through this cool part of the tube as a dark fibril and absorption lines are shifted according to the outflow – this can be the origin of the Evershed effect.

The theoretical models described above are idealized. Individual features are isolated of the full problem and their properties are explored disregarding the complexity of the real situation. In spite of that, the results of these models can be directly compared to observations. This is an important progress in the modelling of magnetoconvection and also a big challenge to the observers to increase further the resolution and quality of the data.

Acknowledgements

It is a pleasure to acknowledge the hospitality of the organizers of the Summer School. This work was accomplished under the Key Project K1-003-601 of the Academy of Sciences of the Czech Republic and was supported by the grant A3003601 of GA AV ČR.

References

Aballe Villero M.A., 1992, Thesis, Univ. La Laguna.
Abdusamatov K.I., 1970, Soviet Astr. 14/1, 64.
Adjabshirzadeh A. and Koutchmy S., 1980, A&A 89, 88.
Adjabshirzadeh A. and Koutchmy S., 1983, A&A 122, 1.
Albregtsen F. and Maltby P., 1981, Solar Phys. 71, 269.
Beckers J.M. and Schröter E.H., 1968, Solar Phys. 4, 303.
Beckers J.M. and Schröter E.H., 1969, Solar Phys. 10, 284.

Biermann L., 1941, Vierteljahrschr. Astron. Ges. 76, 194.
Bray R.J. and Loughhead R.E., 1964, Sunspots, Chapman and Hall, London.
Bumba V., Hejna L. and Suda J., 1975, Bull. Astr. Inst. Czechosl. 26, 315.
Bumba V. and Suda J., 1980, Bull. Astr. Inst. Czechosl. 31, 101.
Bumba V. and Suda J., 1983, Bull. Astr. Inst. Czechosl. 34, 29.
Casanovas J., Vázquez M. and Bonet J.A., 1974, Urania, No. 279–280.
Chevalier S., 1916, Ann. Obs. Astron. Zô-Sè, Tome IX, B1.
Chitre S.M. and Shaviv G., 1967, Solar Phys. 2, 150.
Choudhuri A.R., 1986, ApJ 302, 809.
Choudhuri, A.R., 1992, in Sunspots: Theory and Observations, J.H. Thomas and N.O. Weiss (eds.), Kluwer, Dordrecht, 243.
Collados M., Martínez-Pillet V., Ruiz Cobo B., del Toro Iniesta J.C. and Vázquez M., 1994, A&A 291, 622.
Cowling T.G., 1934, MNRAS 94, 39.
Danielson, R., 1964, ApJ 139, 45.
Degenhardt D. and Wiehr E., 1991, A&A 252, 821.
Degenhardt D. and Lites B.W., 1993a, ApJ 404, 383.
Degenhardt D. and Lites B.W., 1993b, ApJ 416, 875.
Degenhardt D. and Wiehr E., 1994, A&A 287, 620.
del Toro Iniesta J.C., Tarbell T.D. and Ruiz Cobo B., 1994, ApJ 436, 400.
Ewell, M.W., 1992, Solar Phys. 137, 215.
Grossmann-Doerth U., Schmidt W. and Schröter E.H., 1986, A&A 156, 347.
Hale, G.E., 1908, ApJ 28, 315.
Hofmann J., Deubner F.L., Fleck B. and Schmidt W., 1994, A&A 284, 269.
Hoyle F., 1949, Some Recent Researches in Solar Physics, Cambridge Univ. Press.
Jahn K., 1997, in Advances in the Physics of Sunspots, B. Schmieder, J.C. del Toro Iniesta and M. Vázquez (eds.), ASP Conf. Ser. Vol. 118, 122.
Jahn K. and Schmidt H.U., 1994, A&A 290, 295.
Johannesson A., 1993, A&A 273, 633.
Kitai R., 1986, Solar Phys. 104, 287.
Kneer F., 1973, Solar Phys. 28, 361.
Kopp G. and Rabin D., 1992, Solar Phys. 141, 253.
Koutchmy S. and Adjabshirzadeh A., 1981, A&A 99, 111.
Kusoffsky U. and Lundstedt H., 1986, A&A 160, 51.
Leka K.D., 1997, ApJ 484, 900.
Lites B.W., Scharmer G.B. and Skumanich A., 1990, ApJ 355, 329.
Lites B.W., Bida T.A., Johannesson A. and Scharmer G.B., 1991, ApJ 373, 683.
Mallia E.A. and Petford A.D., 1972, MNRAS 157, 73.
Maltby P., 1992, in Sunspots: Theory and Observations, J.H. Thomas and N.O. Weiss (eds.), Kluwer, Dordrecht, 103.
Maltby P., 1997, in Advances in the Physics of Sunspots, B. Schmieder, J.C. del Toro Iniesta and M. Vázquez (eds.), ASP Conf. Ser. Vol. 118, 91.
Maltby P., Avrett E.H., Carlsson M., Kjeldseth-Moe O., Kurucz R. and Loeser R., 1986, ApJ 306, 284.
Martínez-Pillet V., 1992, Solar Phys. 140, 207.
Martínez-Pillet V., 1997, in Advances in the Physics of Sunspots, B. Schmieder, J.C. del Toro Iniesta and M. Vázquez (eds), ASP Conf. Ser. Vol. 118, 212.
Martínez-Pillet V. and Vázquez M., 1993, A&A 270, 494.
Molowny-Horas R., 1994, Solar Phys. 154, 29.
Muller R., 1973a, Solar Phys. 29, 55.
Muller R., 1973b, Solar Phys. 32, 409.
Muller R., 1976, Solar Phys. 48, 101.
Muller R., 1979, Solar Phys. 61, 297.
Muller R., 1992, in Sunspots: Theory and Observations, J.H. Thomas and N.O. Weiss (eds.), Kluwer, Dordrecht, 175.

Muller R. and Mena B., 1987, Solar Phys. 112, 295.
Obridko V.N., 1975, Soviet Astr. 18, 758.
Obridko V.N. and Staude J., 1988, A&A 189, 232.
Parker E.N., 1979a, ApJ 230, 905.
Parker E.N., 1979b, ApJ 234, 333.
Pizzo J.V., 1986, ApJ 302, 785.
Priest E.R., 1982, Solar Magnetohydrodynamics, Reidel, Dordrecht.
Proctor M.R.E., 1992, in Sunspots: Theory and Observations, J.H. Thomas and N.O. Weiss (eds.), Kluwer, Dordrecht, 221.
Rimmele T.R., 1994, A&A 290, 972.
Rimmele T.R., 1995a, A&A 260, 276.
Rimmele T.R., 1995b, ApJ 445, 511.
Rösch J., 1957, l'Astronomie 71, 129.
Rüedi I., Solanki S.K. and Livingston W., 1995, A&A 302, 543.
Schlichenmaier R., Jahn K. and Schmidt H.U., 1997, in Advances in the Physics of Sunspots, B. Schmieder, J.C. del Toro Iniesta and M. Vázquez (eds.), ASP Conf. Ser. Vol. 118, 140.
Schlüter A. and Temesváry S., 1958, in Electromagnetic Phenomena in Cosmical Physics, B. Lehnert (ed.), IAU Symp. No. 6, Cambridge Univ. Press, 263.
Schmidt W., Hofmann A., Balthasar H., Tarbell T.D. and Frank Z.A., 1992, A&A 264, L27.
Schmidt W. and Balthasar H., 1994, A&A 283, 241.
Shine R.A., Title A.M., Tarbell T.D. and Topka K.P., 1987, Science 238, 1203.
Shine R.A., Title A.M., Tarbell T.D., Smith K. and Frank Z.A., 1994, ApJ 430, 413.
Simon G.W., Brandt P.N., November L.J., Scharmer G.B. and Shine R.A., 1994, in Solar Surface Magnetism, R.J. Rutten and C.J. Schrijver (eds.), Kluwer, Dordrecht, 261.
Sobotka M., 1985, Soviet Astr. 29, 576.
Sobotka M., Bonet J.A. and Vázquez M., 1992, A&A 260, 437.
Sobotka M., Bonet J.A. and Vázquez M., 1993, ApJ 415, 832.
Sobotka M., Bonet J.A. and Vázquez M., 1994, ApJ 426, 404.
Sobotka M., Bonet J.A., Vázquez M. and Hanslmeier A., 1995, ApJ 447, L133.
Sobotka M., Brandt P.N. and Simon G.W., 1997a, A&A 328, 682.
Sobotka M., Brandt P.N. and Simon G.W., 1997b, A&A 328, 689.
Solanki S.K., 1997, in Advances in the Physics of Sunspots, B. Schmieder, J.C. del Toro Iniesta and M. Vázquez (eds.), ASP Conf. Ser. Vol. 118, 178.
Thiessen G., 1950, Observatory 70, 234.
Thomas J.H. and Weiss N.O., 1992, in Sunspots: Theory and Observations, J.H. Thomas and N.O. Weiss (eds.), Kluwer, Dordrecht, 3.
Title A.M., Frank Z.A., Shine R.A., Tarbell T.D. and Topka K.P., 1993, ApJ 403, 780.
Tönjes K. and Wöhl H., 1982, Solar Phys. 75, 63.
Tritschler A. and Schmidt W., 1997, A&A 321, 643.
Vázquez M., 1973, Solar Phys. 31, 377.
Wang H. and Zirin H., 1992, Solar Phys. 140, 41.
Weiss N.O., 1997, in Advances in the Physics of Sunspots, B. Schmieder, J.C. del Toro Iniesta and M. Vázquez (eds.), ASP Conf. Ser. Vol. 118, 21.
Weiss N.O., Brownjohn D.P., Matthews P.C. and Proctor, M.R.E., 1996, MNRAS 283, 1153.
Wiehr E., 1994, A&A 287, L1.
Wiehr E., Koch A., Knölker M., Küveler S. and Stellmacher G., 1984, A&A, 140, 352.
Wiehr E. and Stellmacher G., 1989, A&A 225, 528.
Wiehr E. and Degenhardt D., 1993, A&A 278, 584.
Wiehr E. and Degenhardt D., 1994, A&A 287, 625.
Zirin H. and Wang H., 1989, Solar Phys. 119, 245.
Zwaan C., 1965, Rech. Astr. Obs. Utrecht XVII (4), 1.